Tadeusz MARKOWSKI
Jacek MUCHA
Waldemar WITKOWSKI

FEM ANALYSIS OF CLINCHING JOINT MACHINE'S C-FRAME RIGIDITY

ANALIZA MES SZTYWNOŚCI C-RAMY URZĄDZENIA DO WYTWARZANIA POŁĄCZEŃ PRZETŁOCZENIOWYCH*

This paper presents the results of FEM analysis for clinching joint machine's C-frame. Several versions of frame geometry were accounted for when analyzing the straining of material, including the mass reduction. The purpose of this FEM simulation was to determine the effect of mass reducing material recess on the structure rigidity. ABAQUS software was used to analyze the frame material straining from both the qualitative and quantitative point of view.

Keywords: C-frame deflection, FEM modeling, clinching joints.

W artykule przedstawiono wyniki symulacji MES C-kształtnej ramy urządzenia do montażu połączeń konstrukcji blaszanych. Podczas analizy wytężenia materiału ramy wzięto pod uwagę kilka wariantów wykonania jej geometrii, uwzględniając zmniejszenie masy. Celem symulacji MES było wykazanie wpływu postaci wybrań materiału zmniejszających jej masę na sztywność takiej konstrukcji. Do tak postawionego zadania użyto programu ABAQUS umożliwiającego ilościową i jakościową ocenę wytężenia materiału ramy.

Słowa kluczowe: ugięcie C-ramy, modelowanie MES, połączenia przetłoczeniowe.

1. Introduction

Robot equipped assembly stations are extensively used in the industry branches. These stations are used especially in the automotive industry, where fully automated car body assembly lines equipped available (Fig. 1); these stations are equipped with industry robots and clinching joint machines with or without native material [8, 9, 12].
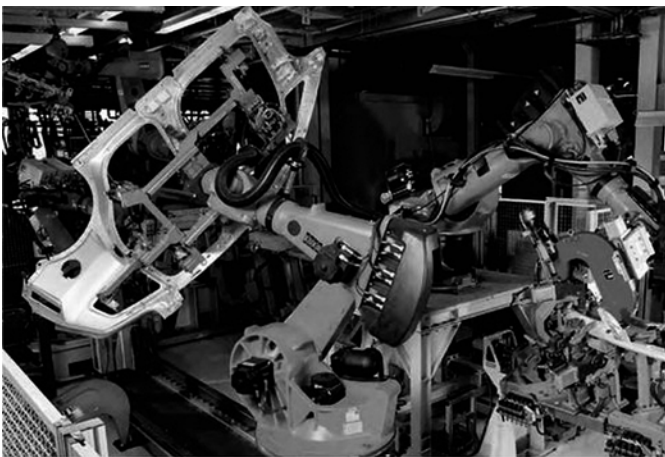

Fig. 1. Automated lateral assembly station for car body element

Joining car body elements is a fully automated process using the industry robot working with high speeds. This high speed work is related with high loads due to a robot path dynamics.

When designing the robot's manipulator movements, energy minimum and time loads are sometimes considered as a target functions to perform these movements at given design and dynamic limitations.

The relation between forces affecting the system and the inertia forces is presented below in the matrix form:

$$H(q)\ddot{q} + h(q,\dot{q}) = P \qquad (1)$$

where:

$H(q)$ – the inertia matrix of an industry robot's manipulator (IRM),

$h(q,\dot{q})$ – matrix of Coriolis centrifugal force and gravity of IRM,

P – vector of generalized moments applied to IRM items [6].

It is reasonable to find a way to reduce unwanted IRM loads. One of possible solutions is to reduce the C-frame mass relatively while preserving its allowed deflection when joining sheet metal pieces.

The devices used both in mobile industry robots and fixed workstations can be equipped with C-frames (Fig. 2). When producing thick joints of sheet metals, the C-frames are replaced with heavy bodies, which due to their mass are used in fixed assembly stations.

Both mobile and fixed solutions can be driven by electric servomotors, pneumatic-hydraulic drives and controlled hydraulic cylinders. The electric servomotors offer the best capabilities of precise control. These drives are available as compact and modular devices of limited own mass. These constructions supplement existing and developing conventional press drives. They are used in highly demanding plastic working industry branches [14,15].

In the plastic working processes it is very important to achieve the adequate rigidity of a forming tool and the ma-

chine body, e.g. the press frame. When these requirements are fulfilled, the produced item form repeatability os preserved [1, 2, 7].
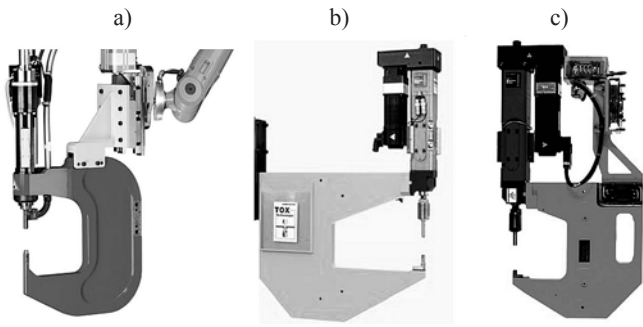

Fig. 2. C-frames used in the industry robot manipulators: a), b) closed design, b) with opening

The purpose of this paper is to present the strength analysis of effect of selected geometry versions of C-frame in the industry robot manipulator producing the thin-walled structures with clinching joints.

The calculations were performed for various frame geometry models at assumed identical maximum joining force and material type. The strength analysis was performed with the finite element method (FEM).

2. The frame deflection effect on tool positioning when forming the joint

The most developed sheet joining methods by local cold pressing include:
– local material restamping using round tools, and
– bonding the sheet metal layers by restamping with local notch [3,12].

For round clinching joints, the identical joint strength is achieved in each radial load direction. The rectangle clinching joints with notch have an irregular form and the joint behaves differently when changing the load direction [10].

From the point of view of the forming tools mating in the plastic working process, preserving the adequate machine body rigidity with its possibly low mass is critical [4].

Small rigidity of support C-frame results in an increased tool axis deviation and low repeatability, i.e. the joint round in its all radial directions.

The tool face deviation due to the force F by angle ϕ in relation to center c results in frame deflection by f (Fig. 3a). The axes of mating tools mounted in the frame are then deviated by angle γ. Due to the C-frame deflection, the base surface position to set the die is deviated, and this in turn changes parameter X value by Δx. The X displacement component affects achieving the clinching joint's bottom of a specified thickness X. The X value of a joint is a measured process parameter, which affects corresponding lock forming in materials being joined [11]. This is critical when joining thin sheet metals, as the joint walls may become drastically thin (Fig. 3b) [13].

For automated workstations, the diagnostic system monitors the machine status, and thus the joining process. Possible deviations from the starting values (standard ones determined in a specified test) in e.g. forming force are indicated on the operator panel (Fig. 4). Sudden change of its value may indicate the friction or fatigue wear of tool.

3. The assumptions of FEM analysis geometry models

When analyzing the rigidity of various frame geometry models we decided to use only fixed external dimensions and variables including mass reduction by implementing internal recesses. The full
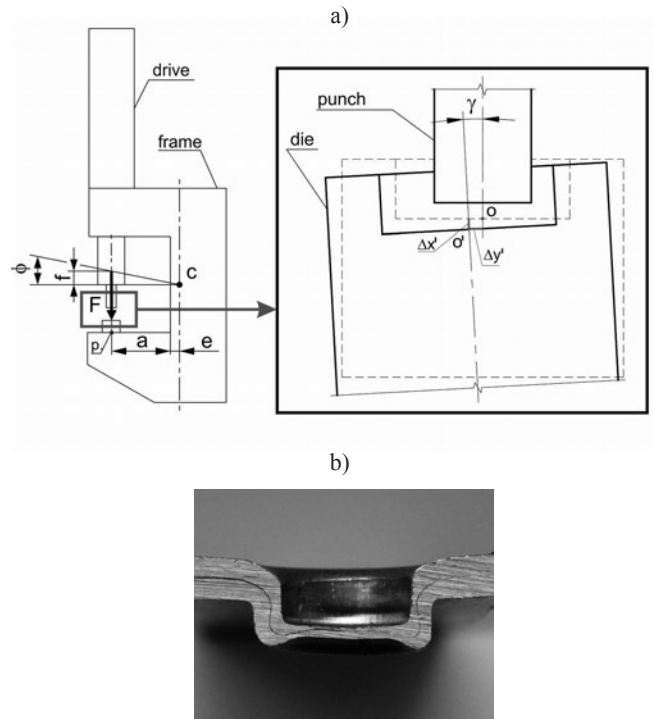

a)

b)

Fig. 3. The effect of frame deflection on positioning and coaxiality of punch-die: a) graphical description, b) joint asymmetry
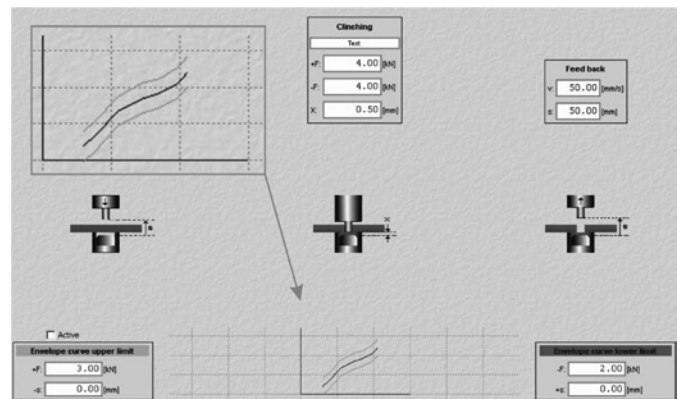

Fig. 4. Example screenshot of servomotor control software's UI dialog box to set parameter X of joint forming
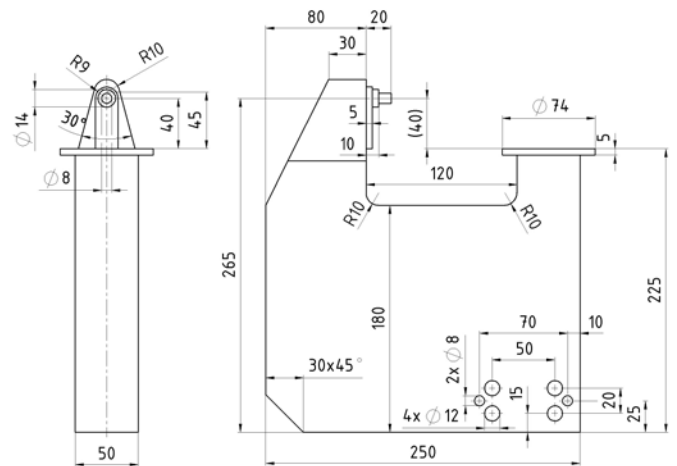

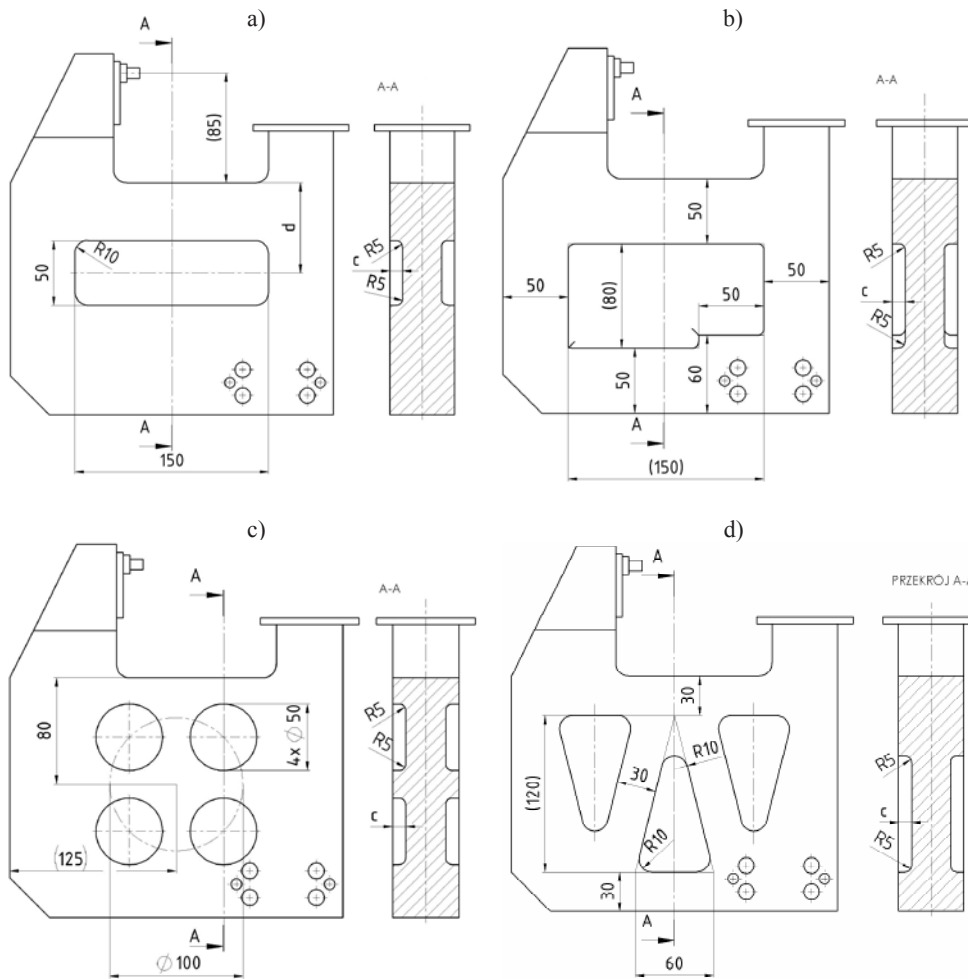Fig. 5. Geometry of an uniform frame — model I

Fig. 6. Geometry of modified frame — models II — VII

Table 1. Opening depth in a modified frame

Variable parameter	C-frame model version						
	M-I	**M-II**	**M-III**	**M-IV**	**M-V**	**M-VI**	**M-VII**
	Fig. 5	Fig. 6a			Fig. 6b	Fig. 6c	Fig. 6d
Recess depth **c** [mm]	0	25	10*	25	10	25	25
*Base distance **d** for model **M-III** is 50, remaining values are 60, 70, 80, 90, 100 [mm]							

Table 2. Frame deflection values for various C-frame models

Axis deflection x 10⁻³ [μm]	C-frame model version						
	M-I	**M-II**	**M-III**	**M-IV**	**M-V**	**M-VI**	**M-VII**
$|\Delta \mathbf{x}|$	435	662	449	604	447	486	515
$|\Delta \mathbf{y}|$	193	214	186	227	185	192	232

frame was a base model (M-I; Fig. 5), for which remaining six were created (Fig. 6). The analysis of opening position effect was additionally performed for model M-III (Fig. 6a and Table 1).

When analyzing the opening position effect on frame deflection, its distance *d* was assumed in range 50 to 100 with 10 mm pitch (Fig.

6a and Table 1). In all models, the external dimensions and thickness were identical, and only the opening geometry in the frame was changed.

Performing the FEM analysis for C-frame loaded with force F allowed us to check how much the change of opening geometry increased the frame deflection. This will allow to perform the opening placement optimization task in the future. The geometry of full frame was taken from the product catalog of the C-frame manufacturer.

4. Modeling the frame load in ABAQUS software

Due to a simple structure, all geometrical models were created directly in MES Abaqus 6.10.1 software and digitized. The base model of full frame included the finite element mesh of 81,000 10-node tetragonal elements; the elements were designated in the program library as C3D10.

The boundary conditions and the external load (as a maximum joining force F on C-frame of these dimensions) were defined in the coordinate system of the model (*x y z*; Fig. 7a). The opening were skipped on the drive mounting flange, and the node displacement limitation on its surface in all directions and rotation limitation in relation to x, y, z axis of the system was assumed. The force F was 50 kN, modulus of elasticity for steel was $E = 2.1 \times 10^5$ MPa, and the Poisson's coefficient was *v*=0.3. The solid model with force application points, the model anchorage points and the mesh generated for this model were presented on Fig. 7a and 7b.

The distribution of stress contour lines reduced based on H-M-H hypothesis and material displacement was observed for specified load force *F* of the C-frame. The analysis was performed as a static one.

The effect of material on the recess geometry on the distribution of stress contour lines reduced based on H-M-H hypothesis including stress concentrators was observed during the straining analysis of the C-frame. The deflection values and the mass change due to machine body material recess geometry was read. The deflection measurement was performed in the C-frame node, on the base surface for die positioning and mounting (Fig. 3a).

Different deflection values (Table 2) were achieved for individual model versions and such a selected measurement point. The example of frame deformation with rectangle through opening at the zoom in factor of 50 was presented on Fig. 8.

When forming the clinching joint, the C-frame absorbs the elastic strain energy W_d, thus achieving the potential energy of eclectically strained body:
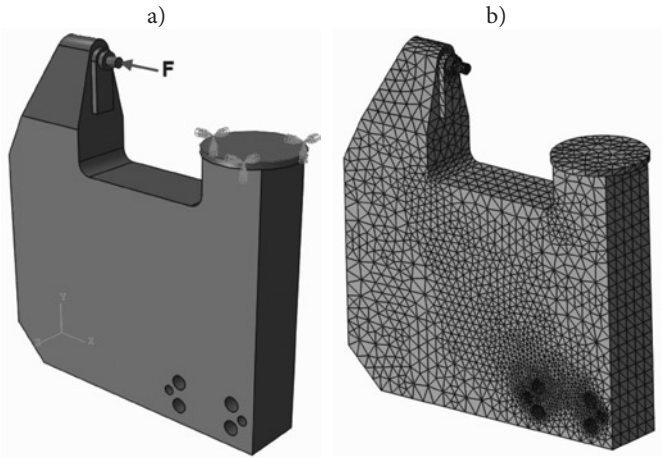
Fig. 7. C-frame, base model view: a) solid model with boundary conditions and external load, and b) discreet model with finite element mesh

Fig. 8. C-frame deformation after maximum forming force load (clinching joint) and its model under load condition (zoom in factor of 50).

$$W_d = \frac{1}{2}\frac{F \cdot f}{10^3}[J] \qquad (2)$$

Where:

W_d – the potential energy of elastically strained frame [Nm],
F – pressure force [N],
f – frame deflection [mm].

The frame rigidity C (the strain resistance) is a quotient of force F and deflection $\Delta x=f$:
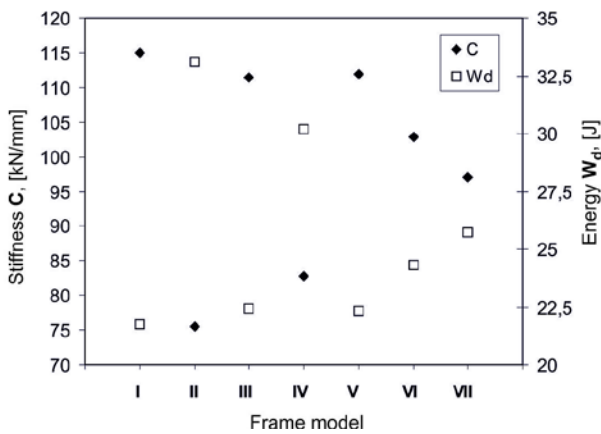

Fig. 9. The relations between frame rigidity and elastic deflection energy
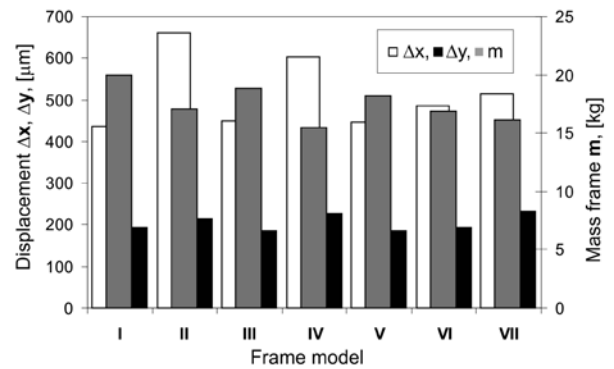

Fig. 10. Mass and displacement changes in the measurement point of frame loaded with force 50 kN

$$C = \frac{F}{\Delta x}, \left[\frac{kN}{mm}\right] \qquad (3)$$

The relations between the rigidity and the frame elastic strain energy (for all models) were presented in Fig. 9. The lower the rigidity (value C), the more the frame absorbs the forming force energy F.

The frame had the highest mass, and thus the highest structure rigidity, and this in turn resulted in the smallest material displacement under load force of 50 kN (Fig. 10 and 11a). The highest mass reduction by 22.5% in relation to a solid frame was achieved for model M-IV. Such a form of frame material recesses (openings) resulted in increasing the frame deflection in x and y direction of the xyz system.

As mentioned earlier, modern control systems enable frame deflection compensation in x axis direction with ±0.01mm accuracy, while it is almost impossible to compensate the deflection component in y direction. The smallest unwanted deflection in y direction was achieved for a frame with recess (model M-V), and the highest for
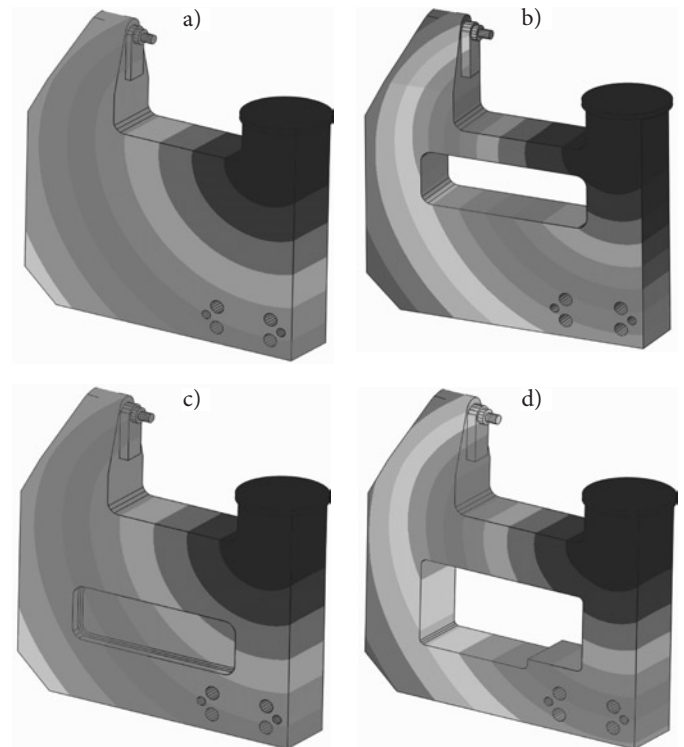

Fig. 11a – d. The distribution of resulting displacement of C-frame for various material recess geometry (models M-I÷M-VII; U_w, mm)
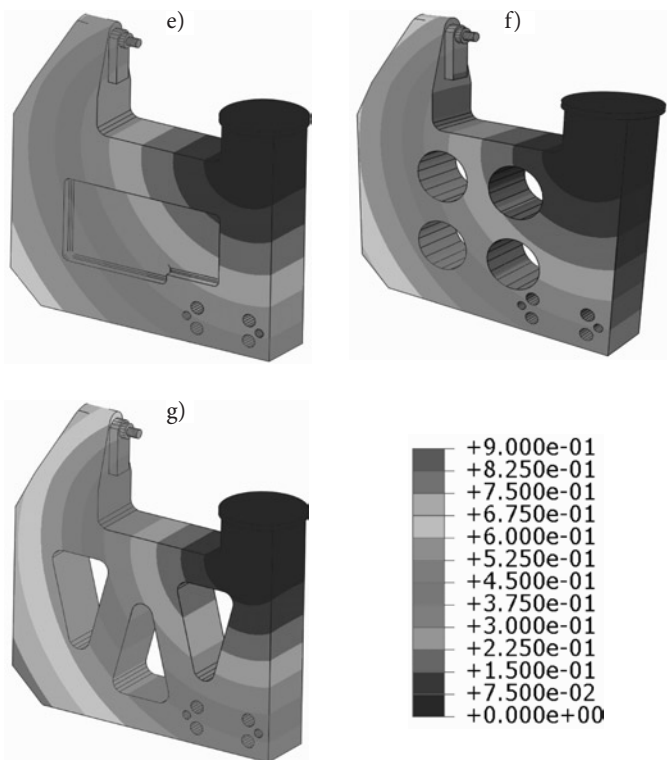
Fig. 11e – g. The distribution of resulting displacement of C-frame for various material recess geometry (models M-I÷M-VII; U_w, mm)

Fig. 12e – g. The distribution of C-frame stress reduced based on H-H-H for various material recess geometry (models M-I÷M-VII; σ_z, MPa)

model M-VII (Fig. 10), which included the discontinuity in form of triangle openings. The highest value of resulting displacements was observed for model M-II (Fig. 11b).

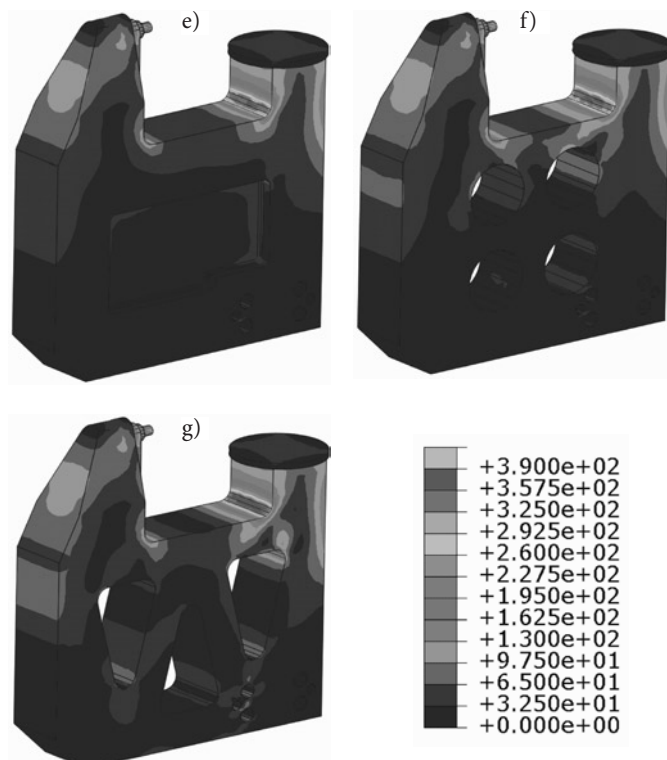For all C-frame models, the highest material straining was located on the internal surface of wall arm radial transition into the remaining part of the body. The strain concentration was lower on internal surfaces of openings (Fig. 12b, d, f, g).

The highest stress was observed in the location of the highest deflectioning load acting the geometrical stress concentrator area in model M-VII (Fig. 13). Therefore, in the future analyses we decided to examine the effect of transition surface radius value (2, Fig. 13) to the stress concentration and value in this area.
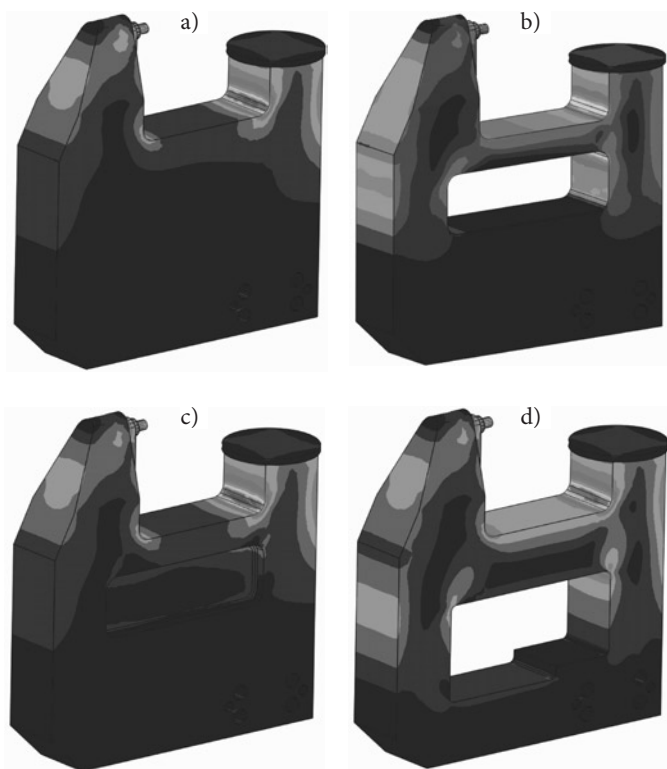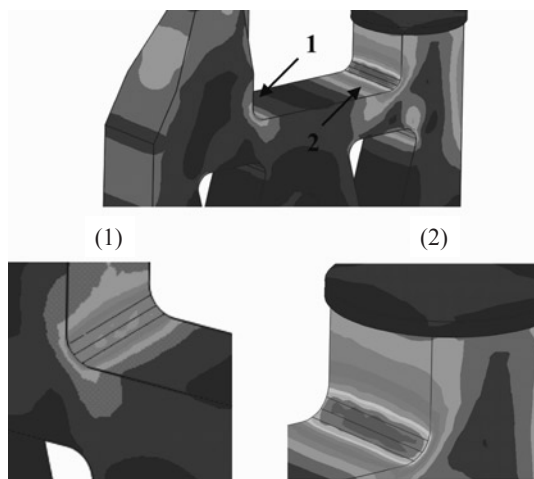

Fig. 13. The stress concentration on the radial surface transition

The change of rectangle opening placement distance (model M-II) significantly affects the behavior of loaded frame. The lowest displacement of the measurement point both in x and y axis of the FEM model coordinate system was achieved for d=100mm from the internal surface of the frame (Fig. 14). The lowest displacement in y axis direction was observed for distance d=60 mm (with d pitch of 10 mm).

Fig. 12a – d. The distribution of C-frame stress reduced based on H-H-H for various material recess geometry (models M-I÷M-VII; σ_z, MPa)
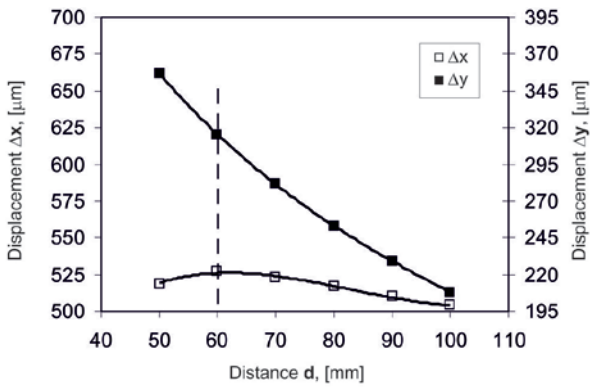
Fig. 14. The displacement in the measurement point of model M-II with various placement of opening
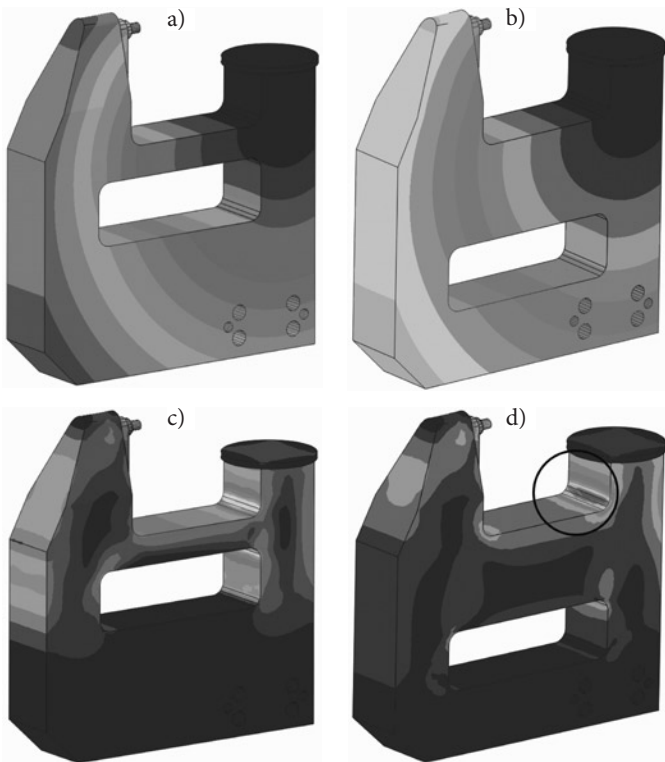

Fig. 15. The effect of opening placement on resulting displacement of frame material (a) and (b) and the distribution of reduced stress contour lines (c) and (d)

The displacement of opening from the C-frame arm base surface by 50mm increased its rigidity, thus increasing stress in the internal corner (the area indicated on Fig. 15d). At the lowest opening distance from this surface (d=50mm) such a created "beam" decreased the stress level in the corner, balancing the frame material stress in this area (Fig. 15c). Thus the base part of the die was deflectioned more (Fig. 15a).

The lowest deflection was observed in the version of C-frame with the opening distant the most from the loading force axis. When forming the joint, the machine body (C-frame) is loaded due to the joint forming. The machine body (including machine tools) state of stress is affected by several factors, and the most important are process forces and inertia forces [16]. Knowing these forces allows to estimate the strength of individual assemblies. The static rigidity of machine bodies is one the most important features affecting the dimension and form accuracy of work pieces [1, 2, 5, 17, 18].
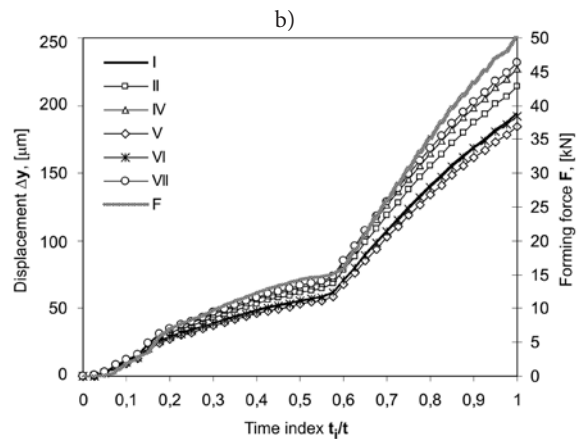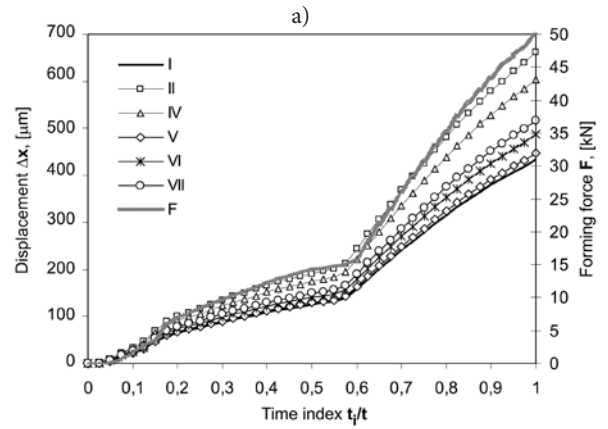

Fig. 16. Material displacement values in the measurement point for variable straining force of C-frame (model M-I÷M-VII): a) Δx, b) Δy

The effect of loading force history on deflection curve was also examined during the frame rigidity FEM analysis. For actual joining force curve (restamping steel sheets, thickness 1mm) the analysis of C-frame material displacement in the measurement point p was performed (Fig. 3a). The response characteristics for such a load was presented on Fig. 16a for Δx and Fi.g 16b for Δy respectively. The curves for model M-III were skipped due to very small slam differences in relation to results achieved for model M-V. For model M-V, the difference between resulting curves of x and y axis displacement for this model and for solid frame was the smallest.

In all frame models, the highest deflection was observed in the final clinching joint forming phase (Fig. 16). When accounting for identical joint forming conditions, the frame used for joint forming should be very rigid, i.e. its deflection characteristics should have the lowest displacement increase.

The final clinching joint forming phase conditions are close to the hydrostatic compression, resulting in a rapid force increase, which easily translates to the C-frame straining.

5. Summary

The "ready to use" C-frame of the clinching joint machine account for an applied load and features the arms of specific structure, enabling easy extension and retraction to and from the joint area. Preserving the adequate tool support rigidity while having relatively low frame mass is critical. The accuracy of tool positioning in the C-frame and frame deflection affect the tool's cutting edge or its coaxiality error. The designed frame can have opening to reduce its mass, but these openings must be of right dimensions, shale and placement.

The forming force curve presents the variable frame load during this process. When designing the body, the most important is to achieve possibly low mass while preserving the highest rigidity.

The conclusions of FEM analysis for displacement of measurement point loaded with force 50 kN are as follows:

– the placement of rectangle frame opening in relation to loading force direction affects the frame rigidity;

– preparing openings (recesses) on all material surface (model M-V) on two sides of frame results in the lowest displacement increase and relatively high mass reduction;

– the highest mass reduction while preserving the deflection change value in a direction lateral to force direction was achieved for model with four openings (model M-VI).

References

1. Brecher C, Esser M, Witt S. Interaction of manufacturing process and machine tool. CIRP Annals - Manufacturing Technology 2009; 58: 588–607.
2. Chodnikiewicz K, Balendra R. The calibration of metal-forming presses. Journal of Materials Processing Technology 2000; 106: 28–33.
3. Di Lorenzo G, Landolfo R. Shear experimental response of new connecting systems for cold-formed structures. Journal of Constructional Steel Research 2004; 3–5: 561–579.
4. Dobrucki W. Podstawy konstrukcji i eksploatacji walcarki. Wydawnictwo Śląsk, 1981.
5. Kosmol J, Wilk P. Próba optymalizacji korpusu obrabiarki z zastosowaniem MES i algorytmu genetycznego. Modelowanie Inżynierskie 2008; 35: 59–66.
6. Kyrylovich V, Bogdanowski M. Zagadnienia zautomatyzowanego planowania ruchów robotów przemysłowych w elastycznych systemach montażowych. Technologia i Automatyzacja Montażu 2009; 1: 18–22.
7. Li YB, Wu DH, Huang MH, Lu XJ. Design of Parallel Bearing Structure for 800MN Forging Press with Consideration of Manufacturing Errors. Applied Mechanics and Materials 2011; 52–54: 2157–2163.
8. Mucha J. Rozwój technik wytwarzania złączy nitowych–nitowanie bezotworowe. Mechanik 2007; 5–6: 454–460.
9. Mucha J. Współczesne techniki łączenia cienkich blach-zaciskanie przez wytłaczanie (Clinching). Mechanik 2007; 11: 932–939.
10. Mucha J. The analysis of rectangular clinching joint in the shearing test. Eksploatacja i Niezawodnosc – Maintenance and Reliability 2011; 3: 45–50.
11. Mucha J, Bartczak B. Analiza procesu łączenia przetłoczeniowego blach. Archiwum Technologii Maszyn i Automatyzacji 2011; 3: 59–68.
12. Mucha J, Kaščák Ľ. Wybrane aspekty kształtowania okrągłych połączeń przetłoczeniowych. Problemy eksploatacji-Maintenance Problems 2010; 4: 29–38.
13. Mucha J, Witkowski W. Możliwości łączenia przetłaczaniem blachy stalowej o grubości poniżej 1 mm. Technologia i Automatyzacja Montażu 2012; 1: 46–49.
14. Plewiński A. Kierunki rozwoju maszyn do obróbki plastycznej. Obróbka Plastyczna Metali 2005; 4: 21–28.
15. Schenke C-C, Wiemer H, Großmann K. Analysis of servo-mechanic drive concepts for forming presses. Production Engineering. Research and Development DOI 10.1007/s11740-012-0391-9.
16. Staniek R, Zielnica J, Gessner A. Wpływ parametrów konstrukcyjnych na stan naprężeń i przemieszczeń w korpusie obrabiarki. Archiwum Technologii Maszyn i Automatyzacji 2010; 4: 159–168.
17. Wang ZX, Yu XL. Stiffness of the overall study for forging hydraulic press. Forging Technology 1990; 1: 1–2.
18. Zhou YD, Chu L, Bi DS. Structural optimization for hydraulic press frame. China Metalforming Equipment & Manufacturing Technology 2008; 2: 90–92.

Prof. Tadeusz MARKOWSKI, Ph.D. (Eng.)
Jacek MUCHA, Ph.D. (Eng.)
Waldemar WITKOWSKI, M.Sc. (Eng.)
Department of Mechanical Engineering
Rzeszow University of Technology
Al. Powstańców Warszawy 8, 35-959 Rzeszów, Poland
E-mails: tmarkow@prz.edu.pl, j_mucha@prz.edu.pl, wwitkowski@prz.edu.pl